Computer-aided mass detection in mammography: False positive reduction via gray-scale invariant ranklet texture features

Matteo Masotti,[a] Nico Lanconelli, and Renato Campanini
Department of Physics, University of Bologna, Viale Berti-Pichat 6/2, 40127, Bologna, Italy

(Received 18 August 2008; revised 18 November 2008; accepted for publication 18 November 2008; published 7 January 2009)

In this work, gray-scale invariant ranklet texture features are proposed for false positive reduction (FPR) in computer-aided detection (CAD) of breast masses. Two main considerations are at the basis of this proposal. First, false positive (FP) marks surviving our previous CAD system seem to be characterized by specific texture properties that can be used to discriminate them from masses. Second, our previous CAD system achieves invariance to linear/nonlinear monotonic gray-scale transformations by encoding regions of interest into ranklet images through the ranklet transform, an image transformation similar to the wavelet transform, yet dealing with pixels' ranks rather than with their gray-scale values. Therefore, the new FPR approach proposed herein defines a set of texture features which are calculated directly from the ranklet images corresponding to the regions of interest surviving our previous CAD system, hence, ranklet texture features; then, a support vector machine (SVM) classifier is used for discrimination. As a result of this approach, texture-based information is used to discriminate FP marks surviving our previous CAD system; at the same time, invariance to linear/nonlinear monotonic gray-scale transformations of the new CAD system is guaranteed, as ranklet texture features are calculated from ranklet images that have this property themselves by construction. To emphasize the gray-scale invariance of both the previous and new CAD systems, training and testing are carried out without any in-between parameters' adjustment on mammograms having different gray-scale dynamics; in particular, training is carried out on analog digitized mammograms taken from a publicly available digital database, whereas testing is performed on full-field digital mammograms taken from an in-house database. Free-response receiver operating characteristic (FROC) curve analysis of the two CAD systems demonstrates that the new approach achieves a higher reduction of FP marks when compared to the previous one. Specifically, at 60%, 65%, and 70% per-mammogram sensitivity, the new CAD system achieves 0.50, 0.68, and 0.92 FP marks per mammogram, whereas at 70%, 75%, and 80% per-case sensitivity it achieves 0.37, 0.48, and 0.71 FP marks per mammogram, respectively. Conversely, at the same sensitivities, the previous CAD system reached 0.71, 0.87, and 1.15 FP marks per mammogram, and 0.57, 0.73, and 0.92 FPs per mammogram. Also, statistical significance of the difference between the two per-mammogram and per-case FROC curves is demonstrated by the p-value < 0.001 returned by jackknife FROC analysis performed on the two CAD systems. [DOI: 10.1118/1.3049588]

Key words: mammography, computer-aided mass detection, ranklets, support vector machine, texture, JAFROC

I. INTRODUCTION

In the last decades, many groups have developed computer-aided detection (CAD) systems which facilitate radiologists in early detection of masses on mammograms.[1–3] Two of the main problems encountered in the development of such systems, and not fully solved yet, can be illustrated as follows. First, the majority of CAD systems is dependent on the gray-scale histogram of the mammograms used for their training; as a result, in order to get good performances on different image databases, some parameters must be adjusted.[4–6] Second, as many false positive (FP) marks usually arises when high sensitivity is desired, it is not easy to get good results in terms of sensitivity-specificity trade-off; this is particularly true for mass detection, as many breast parenchymal structures are particularly similar to masses and, therefore, hardly distinguishable.[7]

Our group has recently developed a CAD system having the potential of being independent on the gray-scale histogram of mammograms;[8–10] as a result, it can be trained on one database, then tested on a different one without the need to adjust any parameter. Such a CAD system is based on the ranklet transform, an image processing technique having the remarkable characteristic of being invariant with respect to linear/nonlinear monotonic transformations of the histogram of the image given as input.

As far as discriminating masses from FP marks, one of the techniques that has emerged as particularly helpful in the last years is texture analysis. Some investigations have been performed on CAD systems making use of texture features derived from gray-scale co-occurrence matrices.[11–13] On one hand, this analysis seems to be powerful for detecting masses while reducing the number of FP marks; on the other hand,

however, it is characterized by being dependent on the histogram of the image. Therefore, tuning must be done when switching to a database of images with a different dynamic range and, if invariance with respect to a histogram is desired, one has either to normalize images before computing texture features or choose only those features that are invariant under monotonic gray-scale transformations.[14]

In this article, a CAD system for mass detection is presented. In particular, a new false positive reduction (FPR) module has been added to a previous version of our CAD system,[8–10] this new FPR module being based on texture features computed on ranklet images corresponding to the regions of interest surviving our previous CAD system.[15] The advantage of this new approach is twofold. First, well-known powerful texture features are exploited for reducing FP marks. Second, as a direct consequence of using ranklets, gray-scale invariance is conferred to those features. As two major results, a significant improvement on the performance of the new CAD system over the previous one is achieved; also, owing to the invariance of the entire system to gray-scale transformations, such a CAD system can be trained on a database of analog digitized mammograms, then tested on a different database of full-field digital mammograms without the need to tune any parameter.

II. MATERIALS AND METHODS

II.A. CAD scheme

A schematic block diagram of both our previous and new CAD systems is shown in Fig. 1.

The detection module, common to both, is aimed at discriminating abnormal from normal tissue. This is achieved by first submitting the original mammogram to the predetection step, where regions more likely to be abnormal are enhanced by means of image processing techniques, such as filtering, thresholding, and morphological operators. The resulting regions are cropped at different scales by means of overlapping square windows, then resized to 64×64 pixels.[16] The resized crops are fed as inputs to the ranklet transform, an image transformation similar to the wavelet transform,[17] yet invariant to linear/nonlinear monotonic gray-scale transformations of the original image.[8–10] Finally, the set of ranklet images that results from the ranklet transformation of each crop is classified as corresponding to abnormal or normal tissue by means of a first-level support vector machine (SVM) classifier. At the end of the detection module, a high mass detection rate, together with a high number of FP marks, is generally achieved.

In order to reduce the number of FP marks while maintaining the highest mass detection rate possible, a ranklet FPR (i.e., RFPR) module was implemented so far; see the left branch of the schematic block diagram shown in Fig. 1. Each region surviving the detection module was encoded by means of the ranklet transform into a set of ranklet images, then classified as representative of a true positive (TP) or FP finding by means of a second-level SVM classifier. At the end of this previous version of our CAD system (RFPR CAD system, hereafter), a high mass detection rate, together with a reasonable number of FP marks, was generally achieved.

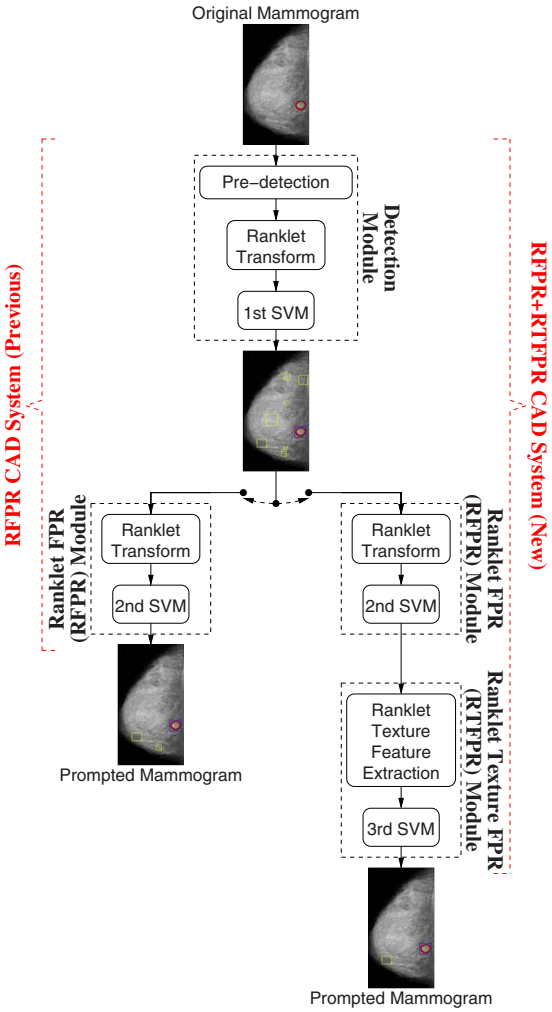

FIG. 1. Schematic block diagram of both the previous RFPR and new RFPR+RTFPR CAD systems.

In this work, with the intention of reducing the number of FP marks surviving the RFPR CAD system even more, an additional ranklet texture FPR (i.e., RTFPR) module is proposed; see the right branch of the schematic block diagram shown in Fig. 1. For each region surviving at the detection and RFPR modules, a set of texture features is extracted from the corresponding ranklet images (hence, ranklet texture features[15]) and further classified as representative of a TP or FP finding by means of a third-level SVM classifier. The rationale behind this new version of our CAD system (RFPR+RTFPR CAD system, hereafter) is twofold. First, a visual inspection of FP marks surviving the RFPR CAD system seems to indicate that texture plays a relevant role in their characterization. Second, being invariant to linear/nonlinear monotonic gray-scale transformations of the original image, the process of encoding regions of interest into ranklet images is crucial, since it allows the RFPR CAD system to be run with similar performances also on mammograms having a dynamic range completely different from that used for training; for instance, as it will be shown in the

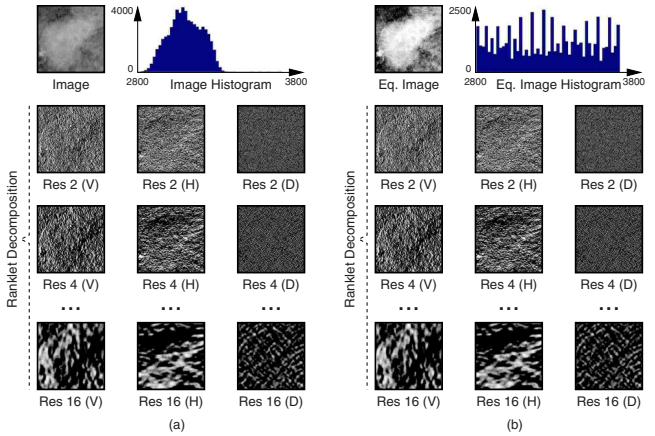

FIG. 2. Ranklet transform, invariance to linear/nonlinear monotonic gray-scale transformations of the original image. Ranklet decomposition of an image (a) and its histogram-equalized version (b) from resolution 2 up to 16. Regardless of the images' gray-scale histogram, the resulting ranklet decompositions are nearly identical.

following, the RFPR CAD system can be trained on analog and tested on digital mammograms without the need of any specific parameters being adjusted. Therefore, in order to use textural information, but at the same time to continue exploiting the gray-scale invariance of the ranklet transform, the RFPR+RTFPR CAD system makes use of a set of ranklet texture features that is calculated directly from the ranklet images corresponding to each region of interest.

II.B. Ranklet transform

As shown in Fig. 1, the regions surviving the detection module are encoded in the RFPR module of both the RFPR and RFPR+RTFPR CAD system by means of the ranklet transform for further analysis through SVM classification; an identical approach is adopted by the detection module itself.

By applying the ranklet transform to an image I, multiresolution, orientation-selective, and nonparametric analysis is performed.[8–10] As a result of this transform, a number $n_{RI}=n_R\times n_O=n_R\times 3$ of ranklet images RI is produced, n_R and $n_O=3$ being the number of resolutions and orientations (i.e., vertical, horizontal, and diagonal) at which the analysis is performed, respectively; also, as ranklet images are derived from the relative rank of the pixels of I, rather than their gray-scale values, they are nonparametric, hence very robust to linear/nonlinear monotonic gray-scale transformations of the original image. As an example, Fig. 2 shows a typical ranklet decomposition and how correspondent ranklet images obtained by decomposing a region and its histogram-equalized version (i.e., nonlinear monotonic gray-scale transformation of the original image) are nearly identical. The reader interested in a more detailed description of the ranklet transform is referred to our previous works dealing with that topic.[8–10]

As for the detection and RFPR modules discussed herein, each region is decomposed into $n_R=4$ resolutions, according to what is discussed in one of our previous works,[8] in fact, this choice is as arbitrary as reasonable, since it spans over a large range of resolutions, from fine to coarse. The resulting $n_{RI}=12$ ranklet images are then linearized into a 1×1428 ranklet feature vector invariant to linear/nonlinear monotonic gray-scale transformations of the original image and used to discriminate through SVM classification between abnormal/normal regions (i.e., detection module) and TP/FP findings (i.e., RFPR module).

II.C. Ranklet texture features

In the RTFPR module of the presented CAD system, the ranklet images corresponding to the regions surviving the detection and RFPR modules are used as a starting point to calculate a number of ranklet texture features; see Fig. 1.

For each ranklet image RI derived from the ranklet decomposition at different resolutions and orientations of an image I, the texture feature extraction step calculates 11 texture features,[15] these features being quite common in the image processing community, as first proposed by Haralick *et al.*,[11] then used for mammographic CAD as well.[12,13] As a result of the texture feature extraction step, each ranklet image RI is encoded by means of a 1×11 texture feature vector; an image I is hence encoded by a texture feature vector obtained by concatenating a number of 1×11 texture feature vectors equal to the number of ranklet images resulting for its ranklet decomposition. Also, being invariant to linear/nonlinear monotonic gray-scale transformations of the original image,[8–10] any texture feature calculated from one of such ranklet images (see Fig. 2) is invariant as well. For more details on ranklet texture features, the interested reader is referred to our previous work dealing with that topic.[15].

As far as the RTFPR module discussed herein, the regions surviving the detection and RFPR modules are decomposed into $n_R=4$ resolutions; hence, they result in a 1×132 ranklet texture feature vector invariant to linear/nonlinear monotonic gray-scale transformations of the original image, namely, a 1×11 texture feature vector for each one of the $n_R=4$ resolutions and $n_O=3$ orientations; these ranklet texture feature vectors are used to discriminate through SVM classification between TP/FP findings.

II.D. SVM classification

SVM is the classification technique adopted in the detection module of both the RFPR and RFPR+RTFPR CAD system to assign a class membership (i.e., abnormal/normal tissue) to the ranklet feature vectors corresponding to the regions found by the predetection step; in the RFPR module of both the RFPR and RFPR+RTFPR CAD systems, SVM is used to assign a class membership (i.e., TP/FP finding) to the ranklet feature vectors corresponding to the regions surviving the detection module; finally, in the RTFPR module of the RFPR+RTFPR CAD system, SVM is used to assign a class membership (i.e., TP/FP finding) to the ranklet texture feature vectors corresponding to the regions surviving the detection and RFPR modules.

Two phases are involved in SVM classification: (1) training of the SVM classifier on feature vectors with known class memberships, and (2) testing of the SVM classifier on

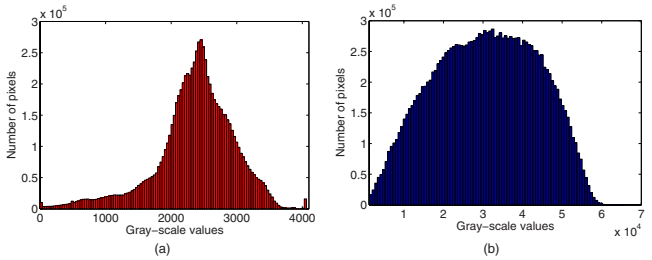

FIG. 3. Difference between the gray-scale dynamics used for training and test both the previous RFPR and new RFPR+RTFPR CAD systems: average gray-scale histogram of analog digitized DDSM mammograms used for training (a) and full-field digital in-house mammograms used for test (b).

feature vectors not used for training. In the context of two-class classification problems, SVM is a learning system that uses an optimal hyperplane to separate the sets of feature vectors into two classes, this hyper-plane being designed during the training phase as the one with the maximum margin of separation between the two classes. SVM classification is a well-known technique and a detailed mathematical formulation of its algorithm can be found by the interested reader in the literature.[18]

II.E. Data

In order to stress the rationale behind the proposed approach (i.e., being able to use textural information, but continuing to exploit the gray-scale in-variance provided by the ranklet transform), training of both the RFPR and RFPR +RTFPR CAD system is performed on mammograms having a gray-scale dynamic completely different from that used for test. To this purpose, training is carried out on analog digitized mammograms taken from the digital database for screening mammography (i.e., DDSM), whereas testing is carried out on full-field digital mammograms taken from an in-house database. An example of the difference between their gray-scale range is given in Fig. 3, where it is possible to notice how their dynamic range is different, namely, more than one order of magnitude on average. Visual appearance of the two databases is different as well: by looking at Fig. 4, in fact, full-field digital mammograms present a wider dynamic range than analog digitized mammograms, this allowing one to perceive a better contrast; furthermore, tissue close to the skin and the nipple can be observed on the former, whereas it is barely visible on the latter.

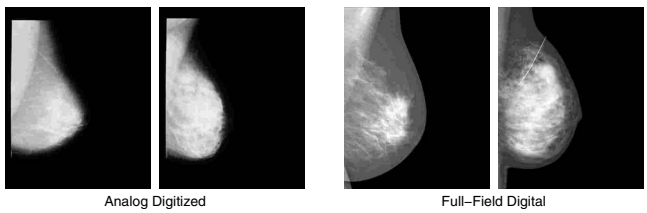

FIG. 4. Analog digitized DDSM mammograms and full-field digital in-house mammograms provided as inputs to the CAD system. Digital mammograms present a wider dynamic range, which allows one to perceive a better contrast. Also, tissue close to the skin and the nipple can be observed well on digital mammograms, whereas it is barely visible on analog mammograms.

In such a situation, when gray-scale-dependent parameters are used in a CAD system, one should act in some way to get the same performance on the two databases. One could either normalize the gray scale of the two databases, or adjust some parameters to get the same results. Unfortunately, it is not easy to normalize the histogram of the images in a reliable and robust way, as often a unique transformation that can map the gray-scale range of one database into the other does not exist. On the other hand, it could be time-consuming and not very effective to manually tune some parameters, given that one should check the performance of the tuning on a test set extracted from the second database. Conversely, owing to the invariance to linear/nonlinear monotonic gray-scale transformations of the proposed CAD system, all the aforementioned procedures can be skipped.

In the present work, training of the first-level SVM classifier (see the detection module of both the RFPR and RFPR+RTFPR CAD system in Fig. 1) is performed with ranklet feature vectors corresponding to 251 masses and 1250 normal crops extracted by analog digitized DDSM mammograms. After training is completed, the detection module is run on 292 cancer and 288 normal analog digitized DDSM mammograms, those mammograms being distinct from the previous ones. TP and FP findings surviving the detection module are fed into the ranklet transform; then, the resulting ranklet feature vectors are used to train the second-level SVM (see the RFPR module of both the RFPR and RFPR+RTFPR CAD systems in Fig. 1). Finally, after training of the second-level SVM is completed, the detection and RFPR modules are run on a further distinct set of 292 diseased and 288 normal analog digitized DDSM mammograms; TP and FP findings surviving the detection and RFPR modules are fed into the ranklet transform; then, ranklet texture features are calculated and used to train the third-level SVM (see the RTFPR module of the RFPR+RTFPR CAD system in Fig. 1). After being trained on analog digitized DDSM mammograms, testing of both the RFPR and RFPR +RTFPR CAD systems is carried out on full-field digital mammograms, namely, 196 diseased mammograms with one mass each (i.e., 100 cases) and 688 normal mammograms (i.e., 172 cases). Full-field digital mammograms are taken from various IMS Giotto Image MD units (Internazionale Medico Scientifica, Bologna, Italy). They are characterized by having an 85 μm pixel and a dynamic range completely different from that of the analog digitized ones. Lesions' locations have been marked by expert radiologists and collected, together with images.

II.F. Performance evaluation

Performance evaluation of both the RFPR and RFPR +RTFPR CAD systems is assessed by using free-response operating characteristic (FROC) curve analysis, namely, a plot showing the mass detection sensitivity as a function of the average number of FP marks per mammogram.[19] Mass detection sensitivity (sensitivity, hereafter) is calculated on a

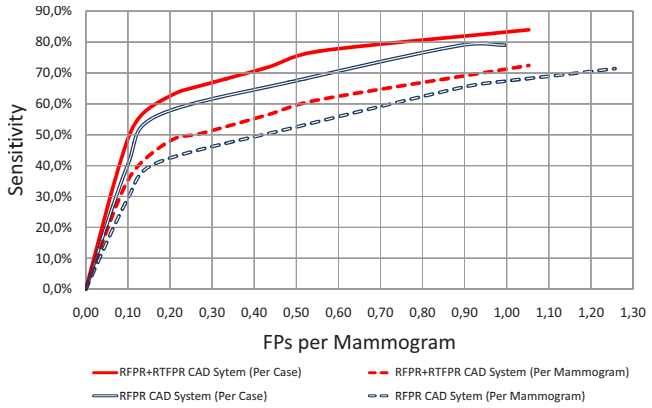

FIG. 5. Per-mammogram and per-case FROC curve analysis of both the previous RFPR and new RFPR+RTFPR CAD systems. FPs per mammogram are reported at different sensitivities.

per-mammogram and per-case basis: in the first case, it is calculated as the percentage of masses detected individually by the CAD system, over the total number of masses marked by the radiologist on the test set's diseased mammograms; in the second case, it is calculated as the percentage of masses detected in either or both the cranio-caudal and medio-lateral oblique views by the CAD system, over the total number of the test set's diseased cases. At a given sensitivity, the average number of FP marks per mammogram (FPs per mammogram, hereafter) is calculated by counting, on the test set, the average number of marks prompted by the CAD system per normal mammogram. As in this work two CAD systems are compared; up to four FROC curves are obtained, namely, a per-mammogram and a per-case FROC curve for each one. In order to estimate the statistical significance of the difference between the two per-mammogram and per-case FROC curves, the jackknife FROC (i.e., JAFROC) method is adopted;[20] in particular, version 2.3 of Chakraborty's JAFROC software is used. A figure of merit to quantify the performance of each FROC is reported, this being a nonparametric estimator of the area under the FROC curve returned from the JAFROC software; more details about the meaning of this estimator can be found in the literture.

III. RESULTS AND DISCUSSION

In Fig. 5, the per-mammogram and per-case FROC curve analysis of both the RFPR and RFPR+RTFPR CAD systems is shown. As a result of the introduction of ranklet texture features, a performance improvement is evidenced, this improvement being even clearer in the range that goes from 0.2 to 0.5 FP marks per mammogram; this is extremely important, as the operating point of clinical CAD systems is often positioned within this range. In Table I, a summary of the FPs per mammogram survived at several per-mammogram and per-case sensitivities is reported, together with the corresponding FP reduction provided by the RFPR+RTFPR over the RFPR approach. Statistical significance of the difference between the two per-mammogram and per-case FROC curves is shown in Table II. Finally, Fig. 6 shows some visual examples of FP marks eliminated by the RTFPR

TABLE I. Summary of the per-mammogram and per-case FROC curve analysis for both the previous RFPR and new RFPR+RTFPR CAD systems. For the two CAD systems, FPs per mammogram and FP reduction are reported at different per-mammogram and per-case sensitivities.

		FPs per mammogram		
	Sensitivity	RFPR CAD system	RFPR+RTFPR CAD system	FP reduction
Per mammogram	60%	0.71	0.50	30%
	65%	0.87	0.68	22%
	70%	1.15	0.92	20%
Per case	70%	0.57	0.37	35%
	75%	0.73	0.48	34%
	80%	0.92	0.71	23%

module. Two typical classes of FP marks are eliminated: (1) signals arising from superposition of breast structures and (2) FP marks in dense breasts. The first class is very common for many types of breasts and is due to the overlapping of breast tissues (or calcified vessels) projected on the planar image; overlapped tissue can resemble in some cases the spiculae typical of infiltrating cancers and, in this case, texture analysis is very useful to separate these structures from spiculated lesions. The second class is more subtle, as the fibroglandular tissue that can produce FP marks is much more widespread on dense breasts; also in this case, texture analysis could help in eliminating FP marks. However, when texture features are gray-scale-dependent, it is not easy to adjust FPR parameters to get a good performance for any type of breasts. Our approach facilitates the rejection of FP marks, as it does not depend on the histogram of the image; hence, it could be optimized for every type of mammogram coming from every type of mammographic unit, both analog and digital.

IV. CONCLUSIONS

By testing without adjusting parameter both the RFPR and RFPR+RTFPR CAD system on mammograms having a gray-scale dynamic completely different from that used for training (i.e., analog digitized DDSM mammograms for training, full-field digital in-house mammograms for testing), the invariance to gray-scale variations of the two CAD systems is emphasized. As far as the higher FPR achieved by

TABLE II. JAFROC analysis of both the previous RFPR and new RFPR+RTFPR CAD systems. For the two CAD systems. JAFROC's figure of merit and p-value associated with the statistical significance of the difference between the two figures of merit are reported on per-mammogram and per-case basis.

	JAFROC's figure of merit		
	RFPR CAD system	RFPR+RTFPR CAD system	p-value
Per mammogram	0.51	0.56	<0.001
Per case	0.57	0.63	<0.001

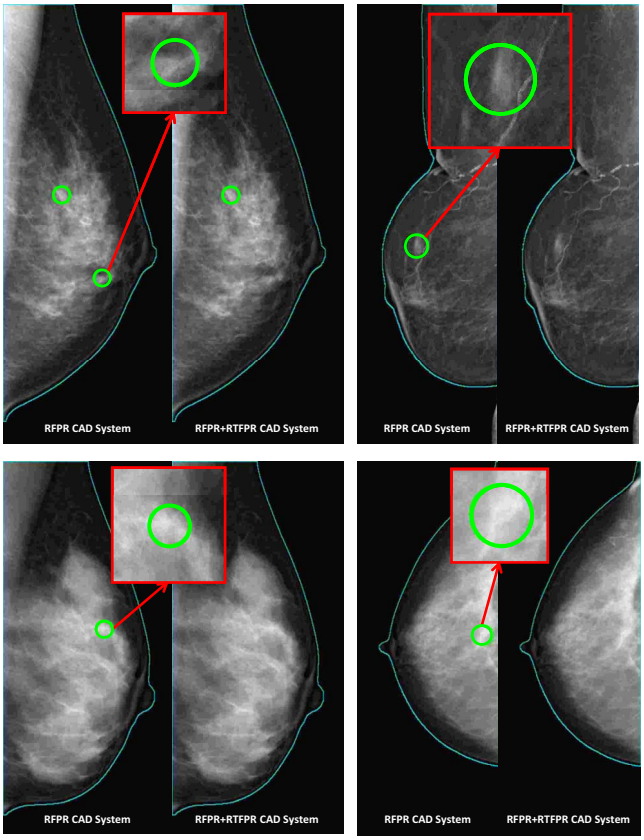

FIG. 6. Visual analysis of some FP marks rejected by the RTFPR module: FP marks caused by the overlapping of breast tissues in fatty breasts (top) and FP marks in dense breasts (bottom).

the RFPR+RTFPR over the RFPR CAD system, this is demonstrated by the FROC curve analysis carried out on them. Also, the difference between the two per-mammogram and per-case FROC curves is revealed to be statistically significant according to the p-value <0.001 returned by JAFROC analysis.

[a]Author to whom correspondence should be addressed. Telephone: +39 051 2095136; Fax: +39 051 2095047; Electronic-mail: masotti@bo.infn.it

[1]M. J. Morton, D. H. Whaley, K. R. Brandt, and K. K. Amrami, "Screening mammograms: Interpretation with computer-aided detection-prospective evaluation," Radiology **239**(2), 373–383 (2006).
[2]J. M. Ko, M. J. Nicholas, J. B. Mendel, and P. J. Slanetz, "Prospective assessment of computer-aided detection in interpretation of screening mammography," AJR, Am. J. Roentgenol. **187**(6), 1483–1491 (2006).
[3]M. Gromet, "Comparison of computer-aided detection to double reading of screening mammograms: Review of 231, 221 mammograms," AJR, Am. J. Roentgenol. **190**(4), 854–859 (2008).
[4]L. Li, R. A. Clark, and J. A. Thomas, "Computer-aided diagnosis of masses with full-field digital mammography," Acad. Radiol. **9**(1), 4–12 (2002).
[5]J. Wei, B. Sahiner, L. M. Hadjiiski, H. P. Chan, N. Petrick, M. A. Helvie, M. A. Roubidoux, J. Ge, and C. Zhou, "Computer-aided detection of breast masses on full field digital mammograms," Med. Phys. **32**(9), 2827–2838 (2006).
[6]J. Ge, B. Sahiner, L. M. Hadjiiski, H. P. Chan, J. Wei, M. A. Helvie, and C. Zhou, "Computer aided detection of clusters of microcalcifications on full field digital mammograms," Med. Phys. **33**(8), 2975–2988 (2005).
[7]D. Gur, J. S. Stalder, L. A. Hardesty, B. Zheng, J. Wei, J. H. Sumkin, D. M. Chough, B. E. Shindel, and H. E. Rockette, "Computer-aided detection performance in mammographic examination of masses: Assessment," Radiology **33**(233), 418–423 (2004).
[8]M. Masotti, "A ranklet-based image representation for mass classification in digital mammograms," Med. Phys. **33**(10), 3951–3961 (2006).
[9]M. Masotti, "Exploring ranklets performances in mammographic mass classification using recursive feature elimination," in *Proceedings of the 16th IEEE International Workshop on Machine Learning for Signal Processing*, Maynooth, Ireland, 2006, pp. 265–270.
[10]R. Campanini, E. Angelini, E. Iampieri, N. Lanconelli, M. Masotti, and M. Roffilli, "A ranklet-based CAD for digital mammography," in *Proceedings of the 8th International Workshop on Digital Mammography*, Manchester, UK, 2006, pp. 340–346.
[11]R. Haralick, K. Shanmugam, and I. Dinstein, "Textural features for image classification," IEEE Trans. Syst. Man Cybern. **3**, 610–621 (1973).
[12]R. Xu, X. Zhao, X. Li, and C. I. Chang, "Target detection with improved image texture feature coding method and support vector machine," Int. J. Intel. Technol. **1**(1), 47–56 (2006).
[13]Y. T. Wu, J. Wei, L. M. Hadjiiski, B. Sahiner, C. Zhou, J. Ge, J. Shi, Y. Zhang, and H. P. Chan, "Bilateral analysis based false positive reduction for computer-aided mass detection," Med. Phys. **34**(8), 3334–3344 (2007).
[14]R. Bellotti, F. De Carlo, S. Tangaro, G. Gargano, G. Maggipinto, M. Castellano, R. Massafra, D. Cascio, F. Fauci, R. Magro, G. Raso, A. Lauria, G. Forni, S. Bagnasco, P. Cerello, E. Zanon, S. C. Cheran, E. Lopez Torres, U. Bottigli, G. L. Masala, P. Oliva, A. Retico, M. E. Fantacci, R. Cataldo, I. De Mitri, and G. De Nunzio, "A completely automated CAD system for mass detection in a large mammographic database," Med. Phys. **33**(8), 3066–3075 (2006).
[15]M. Masotti and R. Campanini, "Texture classification using invariant ranklet features," Pattern Recogn. Lett. **29**(14), 1980–1986 (2008).
[16]R. Campanini, D. Dongiovanni, E. Iampieri, N. Lanconelli, M. Masotti, G. Palermo, A. Riccardi, and M. Roffilli, "A novel featureless approach to mass detection in digital mammograms based on Support Vector Machines," Phys. Med. Biol. **49**(6), 961–975 (2004).
[17]E. Angelini, R. Campanini, E. Iampieri, N. Lanconelli, M. Masotti, and M. Roffilli, "Testing the performances of dierent image representations for mass classification in digital mammograms," Int. J. Mod. Phys. C **17**(1), 113–131 (2006).
[18]V. Vapnik, *Statistical Learning Theory* (Wiley, New York, 1998).
[19]P. C. Bunch, J. F. Hamilton, G. K. Sanderson, and A. H. Simmons, "A free response approach to the measurement and characterization of radiographic observer performance," J. Appl. Photogr. Eng. **4**, 166–171 (1978).
[20]D. P. Chakraborty and K. S. Berbaum, "Observer studies involving detection and localization: Modeling, analysis, and validation," Med. Phys. **31**(8), 2313–2330 (2004).